8-1-2020

A collocation method via the quasi-affine biorthogonal systems for solving weakly singular type of Volterra-Fredholm integral equations

Mutaz Mohammad
Zayed University, mutaz.mohammad@zu.ac.ae

Carlo Cattani
Università degli Studi della Tuscia Viterbo

Alexandria Engineering Journal (2020) 59, 2181–2191

HOSTED BY

ELSEVIER

Alexandria University

Alexandria Engineering Journal

www.elsevier.com/locate/aej
www.sciencedirect.com

ORIGINAL ARTICLE

A collocation method via the quasi-affine biorthogonal systems for solving weakly singular type of Volterra-Fredholm integral equations

Mutaz Mohammad [a,*], **Carlo Cattani** [b]

[a] *Zayed University, Abu Dhabi, United Arab Emirates*
[b] *Engineering School, DEIM, Tuscia University, Viterbo, Italy*

Received 30 December 2019; revised 23 January 2020; accepted 27 January 2020
Available online 21 February 2020

KEYWORDS

Unitary extension principle;
Tight framelets;
Quasi-affine system;
B-splines;
Weakly singular Volterra-Fredholm integral equations

Abstract Tight framelet system is a recently developed tool in applied mathematics. Framelets, due to their nature, are widely used in the area of image manipulation, data compression, numerical analysis, engineering mathematical problems such as inverse problems, visco-elasticity or creep problems, and many more. In this manuscript we provide a numerical solution of important weakly singular type of Volterra - Fredholm integral equations WSVFIEs using the collocation type quasi-affine biorthogonal method. We present a new computational method based on special *B*-spline tight framelets and use it to introduce our numerical scheme. The method provides a robust solution for the given WSVFIE by using the resulting matrices based on these biorthogonal wavelet. We demonstrate the validity and accuracy of the proposed method by some numerical examples.

1. Introduction

Integral equations arise in many scientific, physics, and engineering problems such as quantum and fluid mechanics [1,2], mathematical economics [3], viscoelastic damping [4], the method to calculate the conformal mapping of a domain [5], the reformulation of radiative heat transfer problems [6], the reformulation of partial differential equations of the Helmholtz equation [7], and many applications in various areas can be found in [8–21].

Much effort has been made for producing numerical methods for solving various types of integral equations. In fact, there are several numerical methods for solving variety of Fredholm and Voltera integral equations, such as Galerkin method, Collocation method, Taylor series, transforming equation to a (non) linear system of algebraic equation, Legendre wavelets, Taylor polynomials and recently Chebyshev polynomials and expansion method [29–37]. Among these methods, for example, authors of [22] used Tau method for solving some type of weakly singular integral equations. A new algorithm produced for solving hyper singular integral equations in [23]. The reproducing kernel and the discrete Galerkin methods have been presented in [24,25]. Many efforts have been made for solving various types that used wavelets can be found in [26–28]. Interested readers should consult the references therein to have a complete picture of it.

* Corresponding author.
E-mail address: Mutaz.Mohammad@zu.ac.ae (M. Mohammad).
Peer review under responsibility of Faculty of Engineering, Alexandria University.

https://doi.org/10.1016/j.aej.2020.01.046
1110-0168

With extensive applications of wavelets in image processing, and physical research, etc., there has already been a rapid development of wavelets in solutions of integral equations. We develop a new method based on a generalized wavelet, or simply tight framelet, systems that generated using set of functions that are not orthonormal bases and based on the quasi-affine setup. The systems are produced to approximate the solution of the WSVFEs with singularities.

Numerical solutions of specific types such as WSVFEs are rarely studied in the literature and solving it is usually not easy. So it is important to provide a solution numerically. Tight framelets have been become an emerging area in many fields of applications and computational sciences (e.g. see [38–43]). These framelets have been getting more attention lately for numerically solving specific type of integral equations [44]. We use a quasi-affine (biorthogonal) tight framelets system generated using special type of B-splines based on the collocation method to numerically solve the weakly singular mixed Volterra - Fredholm integral equation defined by

$$u(x) = f(x) + \int_a^x \frac{\mathcal{B}_1(x,y)}{(x-y)^{\alpha}} u(y)dy + \int_a^b \frac{\mathcal{B}_2(x,y)}{(x-y)^{\beta}} u(y)dy,\ 0<\alpha,\beta<1, \tag{1.1}$$

where $f, \mathcal{B}_1(x,y), \mathcal{B}_2(x,y)$ are known continuous functions, and $u(x)$ is the unknown function to be determined (approximated).

The system we use here is generated by the oblique extension principle (OEP) that introduced in [45,51]. This system provides an approximated solution of high accuracy order. It is different from the papers in the literature that we approximate the exact solution using a redundant system (tight frames). The redundancy of the framelet system entails that a given function can be represented in many ways as a convergent sum. Our framelet representation is one of many. These representations have recently emerged as another powerful tool and popular through the use in numerous applications. One of the major advantages of a redundant systems is that it is implemented by a frame fast transform, which will provide us with a better recovery and high accuracy. Also, redundancy can be viewed as the same idea of removing doubt in signal/function representations. Given a function, we represent it in another system, typically a basis, where its characteristics are more readily apparent in the transform coefficients. However, these representations are typically nonredundant, and thus corruption or loss of transform coefficients can be serious. In fact, this is one of the important reasons that we try to approximate the solution for a given integral equation via framelets in order to facilitate various solution processing tasks. Thus, the right representation is critical if we are to perform our solution task effectively and efficiently.

2. Preliminaries

We recall the preliminary background and notations required for our paper (e.g., see [43,46,47,49]). Let $L^2(\mathbb{R})$ denote the space of all square integrable functions over $\mathbb{R}$, where

$$L^2(\mathbb{R}) = \left\{ f:\mathbb{R}\to\mathbb{R}; \int_{\mathbb{R}} |f|^2 < \infty \right\}.$$

In the construction of a framelet $\Psi = \{\psi^{\ell}, \ell = 1,\ldots,r\}$, it is require to use a "magic" function, called refinable function ϕ, where a compactly supported function $\phi \in L^2(\mathbb{R})$ is said to be refinable if

$$\phi(x) = 2\sum_{k\in\mathbb{Z}} h_0[k]\phi(2x-k), \tag{2.1}$$

for some finite supported sequence $h_0[k] \in \ell_2(\mathbb{Z})$, where $\ell_2(\mathbb{Z})$ is the set of all sequences $h[k]_{k\in\mathbb{Z}}$, such that

$$\sqrt{\sum\nolimits_{k=-\infty}^{\infty} h[k]^2} < \infty.$$

The sequence h_0 is called the *low mask filter* of ϕ.

Definition 2.1 [49]. A system $\mathcal{X}(\Psi) = \{\psi^{\ell}_{j,k}, \ell = 1,\cdots,r\}_{j,k\in\mathbb{Z}}$ of elements in $L^2(\mathbb{R})$ is called a *quasi-affine framelet* system for $L^2(\mathbb{R})$ if the following is hold for constants $A, B > 0$ where

$$A\|f\|^2 \leqslant \sum_{\ell=1}^{r}\sum_{j,k}^{\infty} |\langle f, \psi^{\ell}_{j,k}\rangle|^2 \leqslant B\|f\|^2, \forall f \in L_2(\mathbb{R}), \tag{2.2}$$

and $\psi^{\ell}_{j,k}$ is defined as

$$\psi^{\ell}_{j,k} = \begin{cases} 2^{\frac{j}{2}}\psi^{\ell}(2^j\cdot -k), & if\ j \geqslant J \\ 2^j\psi^{\ell}((2^j\cdot -2^{-J+j}k)), & if\ j < J \end{cases} \tag{2.3}$$

such that

$$\psi^{\ell} = 2\sum_{k\in\mathbb{Z}} h_{\ell}[k]\phi(2\cdot -k), \ell = 1,\cdots,r.$$

The numbers A, B are called frame bounds. If $A = B = 1$, then Ψ is called a quasi-affine tight framelet system for $L^2(\mathbb{R})$. $h_{\ell}[k]$ is called the high mask filter of ϕ.

Note that, usually it is known to define $\psi^{\ell}_{j,k}$ as $2^{\frac{j}{2}}\psi^{\ell}(2^j\cdot -k)$. Therefore, the resulting system is not shift-invariant, whereas Definition 2.1 provides a shift-invariant system instead. Meaning, the change in the definition of $\psi^{\ell}_{j,k}$ converts a non-shift invariant system to a shift-invariant system which is preferred in applications [48]. Note that, a set of functions is said to be τ-shift-invariant if for any $k \in \mathbb{Z}$ and $\psi^{\ell} \in L^2(\mathbb{R})$, we have $\psi^{\ell}(\cdot - \tau k) \in L^2(\mathbb{R})$.

The tight frame system defined in Definition 2.1 is equivalent to the following equation [50],

$$\langle f, g\rangle = \sum_{\ell=1}^{r}\sum_{j,k\in\mathbb{Z}} \langle f, \psi^{\ell}_{j,k}\rangle\langle \psi^{\ell}_{j,k}, g\rangle. \tag{2.4}$$

It follows directly from Eq. (2.4) that for any function $f \in L^2(\mathbb{R})$, we have the following quasi-affine tight framelet representation

$$f = \sum_{\ell=1}^{r}\sum_{j\in\mathbb{Z}}\sum_{k\in\mathbb{Z}} \langle f, \psi^{\ell}_{j,k}\rangle\psi^{\ell}_{j,k}. \tag{2.5}$$

Now, Eq. (2.5) can be truncated as

$$\mathcal{Q}_n f = \sum_{\ell=1}^{r}\sum_{j<n}\sum_{k\in\mathbb{Z}} \langle f, \psi^{\ell}_{j,k}\rangle\psi^{\ell}_{j,k}. \tag{2.6}$$

Note that, $\mathcal{Q}_n f$ can be described by a reproducing kernel Hilbert space which is given by a linear combination of its framelets product such that

$$\mathcal{Q}_n f(x) = \int_{\mathbf{R}} f(y)\mathcal{D}_n(x,y)dy, \tag{2.7}$$

where

$$\mathcal{D}_n(x,y) = \sum_{\ell=1}^{r}\sum_{j<n}\sum_{k\in\mathbb{Z}} \psi^{\ell}_{j,k}(y)\psi^{\ell}_{j,k}(x),$$

is called the kernel of $\mathcal{Q}_n f$.

The Fourier transform of a function $f \in L_1(\mathbb{R})$ (this can be extended to $L_2(\mathbb{R})$) is given by

$$\mathcal{F}(f)(\xi) = \hat{f}(\xi) = \int_{\mathbb{R}} f(x)e^{-ix\xi}dx, \quad \xi \in \mathbb{R}.$$

Similarly, we define the Fourier series for a given sequence $h[k] \in \ell_2(\mathbb{Z})$ by the following

$$\mathcal{F}(h)[\xi] = \hat{h}(\xi) = \sum_{k\in\mathbb{Z}} h[k]e^{-ik\xi}dx, \quad \xi \in \mathbb{R}.$$

We use the truncated representation in Eq. (2.7) to find the numerical solution of a given WSVFE using on the quasi-affine tight framelets system generated by some refinable functions called B-splines, where the B-spline, B_m, of order m is defined by

$$B_m = B_{m-1} * B_1 = \int_{(-1/2,1/2]} B_{m-1}(\cdot - x)dx,$$

where $B_1 = \chi_{(-1/2,1/2]}$ is the indicator function of the set $[-1/2, 1/2)$. Note that, $B_m \in C^{m-2}(\mathbb{R})$ and is a piecewise of polynomials. Some of the B-splines are given in Fig. 1.

3. Quasi-affine tight framelets systems

To have good accuracy, effective approximated solution, and sparse representation for a given integral equation, it is important to have framelets with high vanishing moments. The unitary and oblique extension principles (UEP and OEP) found by Ron and Shen in [51] are methods to construct compactly supported tight framelets with good approximation orders, high vanishing moments and specific properties of smoothness and symmetries [50]. In this section, we use the UEP and OEP for constructing quasi-affine tight framelet systems that will be used for finding the approximated solution of the integral equation at hand. We refer the reader to [45,50] for the general setup of both principles.

Example 3.1 (***System I***). Let $h_0[k] = [\frac{1}{4}, \frac{1}{2}, \frac{1}{4}]$, where $k = -1, 0, 1$, be the low mask filter of $B_2(x)$. Using *Mathematica*, we obtain $h_1[k]$ and $h_2[k]$, so we have the following generators defined by

$$\psi^1(x) = \begin{cases} (-\sqrt{2} + \sqrt{2}x), & 0.5 \leqslant x \leqslant 1, \\ -\sqrt{2}x, & -0.5 \leqslant x < 0.5, \\ (\sqrt{2}1 + \sqrt{2}x), & -1 \leqslant x < -0.5, \\ 0, & Otherwise, \end{cases} \tag{3.1}$$

and

$$\psi^2(x) = \begin{cases} 1 - 3x, & 0 \leqslant x \leqslant 0.5, \\ -1 - x, & -1 \leqslant x \leqslant -0.5, \\ -1 + x, & 0.5 < x \leqslant 1, \\ 1 + 3x, & -0.5 < x < 0, \\ 0, & Otherwise. \end{cases} \tag{3.2}$$

Then, $\mathcal{X}(\Psi)$ forms a quasi-affine tight framelet system for $L^2(\mathbb{R})$. $B_2(x)$ and its quasi-affine tight framelet generators, ψ^1, ψ^2, are depicted in Fig. 2.

Example 3.2 (***System II***). Let $h_0[k] = [\cdots, 0, 0, 0.0625, \mathbf{0.25}, 0.375, 0.25, 0.0625, 0, 0, \cdots]_{[-2,2]}$, where $k = -2, \ldots, 2$, be the low mask filter of $B_4(x)$. Define the high mask filters as follows

$$\begin{cases} h_1[k] = [\cdots,0,0,0625,-0.2500,0.3750,-0.2500,0.0625,0,0,\cdots]_{[-2,2]}, \\ h_2[k] = [\cdots,0,0,0.3749,-0.2500,0.0000,0.2500,-0.3749,0,0,\cdots]_{[-2,2]}, \\ h_3[k] = [\cdots,0,0,0.1531,0.0000,-0.3062,0.0000,0.1531,0,0,\cdots]_{[-2,2]}, \\ h_4[k] = [\cdots,0,0,-0.3750,-0.25000,0.0000,0.2500,0.3750,0,0,\cdots]_{[-2,2]}. \end{cases}$$

Hence, $\mathcal{X}(\Psi)$ is a quasi-affine tight framelet system for $L^2(\mathbb{R})$. The cubic quasi-affine tight framelets functions, ψ^1, ψ^2, ψ^3, and ψ^4, that generated using the UEP, are depicted in Fig. 3.

Example 3.3 (***System III***). Consider the linear B-spline $B_2 = \max(1 - |x|, 0)$. By applying the OEP setup to construct the corresponding framelet system, we have the following generators in frequency domain given by

$$\hat{\psi}^1(\xi) = \tfrac{1}{2\pi}\xi^{-2}\left(-1 + e^{\frac{i\xi}{2}}\right)^4,$$

$$\hat{\psi}^2(\xi) = \tfrac{1}{2\pi\sqrt{6}}\xi^{-2}\left(1 + 4e^{\frac{i\xi}{2}} + e^{i\xi}\right)\left(-1 + e^{\frac{i\xi}{2}}\right)^4.$$

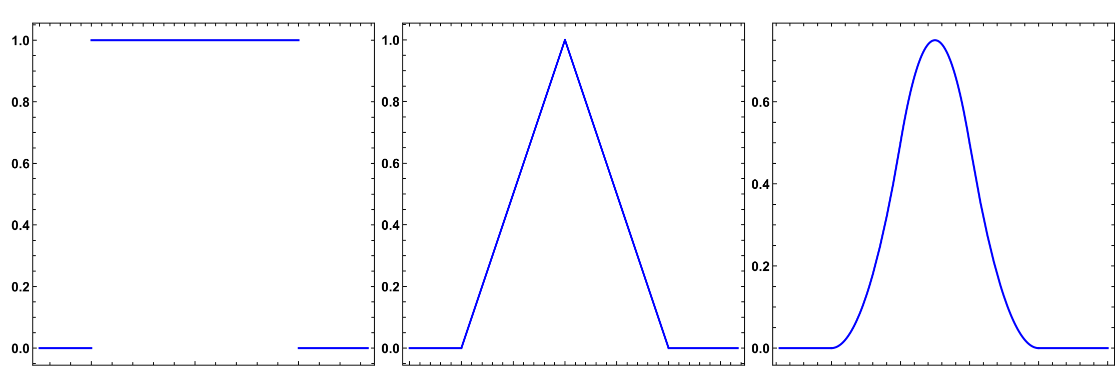

Fig. 1 The refinable functions, B_m, for $m = 1, 2, 3$.

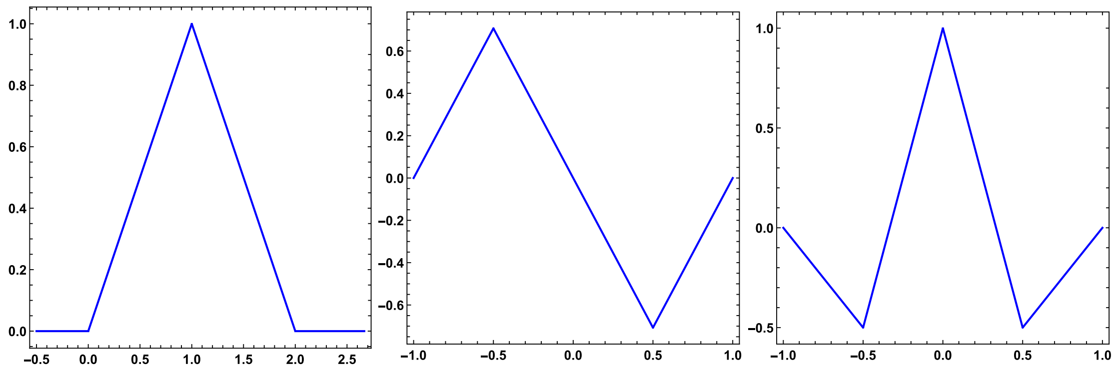

Fig. 2 $B_2(x)$ and its generators of Example 3.1 using the UEP.

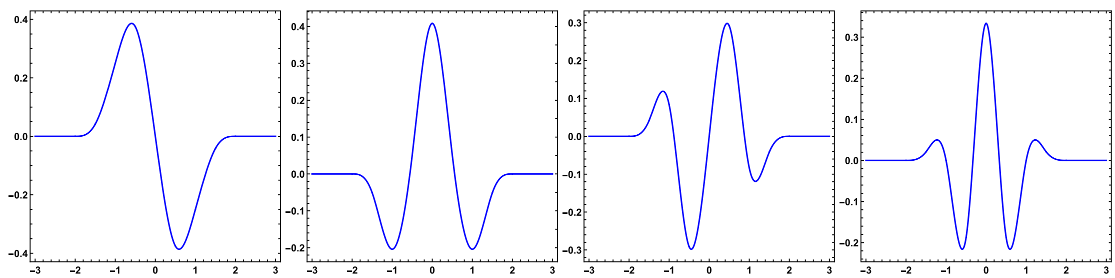

Fig. 3 The generators of Example 3.2 using the UEP.

Then, the system $\mathcal{X}(\Psi)$ forms a quasi-affine tight framelet system for $L^2(\mathbb{R})$. $B_2(x)$ and its quasi-affine tight framelets, ψ^1 and ψ^2, are given in Fig. 4.

Example 3.4 (***System IV***). Consider the cubic B-spline $B_4(x)$. With a similar calculation of constructing the above system in Example 3.3, we define the high mask filters as follows

$$\begin{aligned}
\hat{h}_1(\xi) &= 0.00948145e^{-4i\xi}(1+e^{-2i\xi}+8e^{-i\xi})(-1+e^{i\xi})^4, \\
\hat{h}_2(\xi) &= 0.00829141(1+8e^{-i\xi}+28.52e^{-2i\xi}+8e^{-3i\xi}+e^{-4i\xi}) \\
&\quad (1-e^{-i\xi})^4, \\
\hat{h}_3(\xi) &= 0.00896364(1+8e^{-i\xi}+43.8315e^{-3i\xi}+8e^{-5i\xi} \\
&\quad +e^{-6i\xi}+26.4789(e^{-2i\xi}+e^{-4i\xi}))(1-e^{-i\xi})^4.
\end{aligned}$$

Then, the system $\mathcal{X}(\Psi)$ forms a quasi-affine tight framelet system for $L^2(\mathbb{R})$. The cubic B-spline and its quasi-affine tight framelet generators ψ^1, ψ^2, ψ^3 are depicted in Fig. 5.

4. Matrix assembly using quasi-affine tight framelet systems

In this section, we present the quasi-affine tight framelet expansion method for solving the WSVFIE in Eq. (1.1). By using the truncated expansion

$$\mathcal{Q}_n u(x) = \sum_{\ell=1}^{r} \sum_{j<n} \sum_{k\in\mathbb{Z}} c^{\ell}_{j,k} \psi^{\ell}_{j,k}(x), \tag{4.1}$$

where

$$c^{\ell}_{j,k} = \int_{\mathbb{R}} u_n(x) \psi^{\ell}_{j,k}(x) dx,$$

The results in this section can be concluded using the following algorithm.

Algorithm. The algorithm works in the following way:

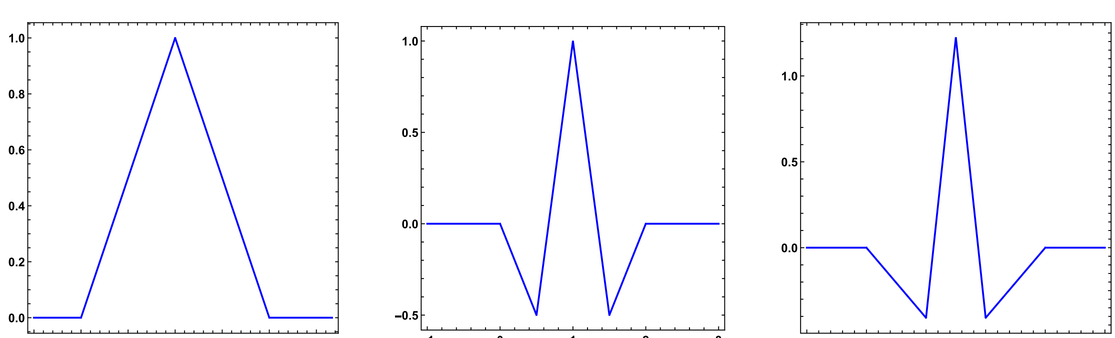

Fig. 4 The B-spline $B_2(x)$ and the corresponding quasi-affine generators via by the OEP.

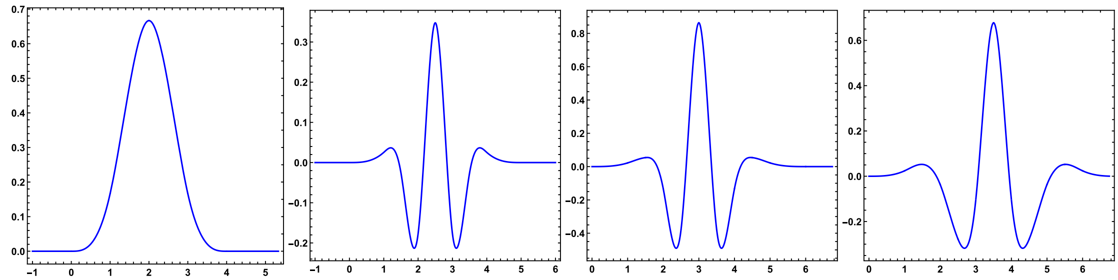

Fig. 5 The B-spline $B_4(x)$ and the corresponding quasi-affine generators via the OEP.

1. We make an *ansatz* for the unknown function, $u(x)$. Here, we choose a suitable collocation points based on the domain and the framelet's support being handled.
2. Approximate $u(x)$ as $\mathcal{Q}_n u(x)$.
3. Substitute $\mathcal{Q}_n u$ to the main problem in Eq. (1.1).
4. Substitute collocation points $\Lambda = \{x_i\}_i$ and create the linear system (assembling the matrix).
5. Solve the resulting system to get the required coefficients.

Consider the WSVFIE in (1.1). Then, from substituting Eq. (4.1) into Eq. (1.1), we have

$$\mathcal{Q}_n u(x) = f(x) + \int_a^x \frac{\mathcal{W}_1(x,t)}{(x-t)^\alpha}\mathcal{Q}_n u(t)dt + \int_a^b \frac{\mathcal{W}_2(x,t)}{(x-t)^\beta}\mathcal{Q}_n u(t)dt.$$

This leads to

$$\sum_{\ell=1}^{r}\sum_{j<n}\sum_{k\in\mathbb{Z}} c_{j,k}^{\ell} m_{j,k}^{\ell}(x) = f(x), \tag{4.2}$$

where

$$m_{j,k}^{\ell}(x) = \psi_{j,k}^{\ell}(x) - \int_a^x \frac{\mathcal{W}_1(x,t)}{(x-t)^\alpha}\psi_{j,k}^{\ell}(t)dt - \int_a^b \frac{\mathcal{W}_2(x,t)}{(x-t)^\beta}\psi_{j,k}^{\ell}(t)dt.$$

By choosing the suitable interpolate nodes $\Lambda = \{x_i\}_i$, which clearly depends on the quasi-affine tight framelet's support and the function domain being handeled, we can collocate the system in Eq. (4.2) as

$$\sum_{\ell=1}^{r}\sum_{j<n}\sum_{k\in\mathbb{Z}} c_{j,k}^{\ell} m_{j,k}^{\ell}(x_i) = f(x_i), \ \textit{for all}\ i \in \Lambda. \tag{4.3}$$

Eq. (4.3) generate a system of linear equations which can be solved for the unknown coefficients. This can be formulated as a matrix form

$$\mathcal{M}\mathcal{D} = \mathcal{L},$$

where, the matrix M and the column vectors F and C are given by

$$\mathcal{M} = \begin{pmatrix} \ddots & \cdots & \ddots \\ \vdots & m_{j,k}^{\ell}(x_i)|_{i,j,k,\ell} & \vdots \\ \ddots & \cdots & \ddots \end{pmatrix},$$

where $i \in \Lambda$ and $\mathcal{L}^T = [\cdots, f(x_i), \cdots]_{i\in\Lambda}$, $\mathcal{D}^T = [\cdots, c_{j,k}^{\ell}, \cdots]_{j,k,\ell}$, $j,k \in \mathbb{Z}, \ell = 1,\ldots,r$, where $\mathcal{L}$ and $\mathcal{D}$ are column vectors of the same order, say, $p \times 1$ and M is an $p \times p$ matrix.

The error function is defined to be

$$\mathcal{E}_n(x) = |u(x) - \mathcal{Q}_n u(x)|, \quad x \in [a,b],$$

and the absolute error for this formulation is defined by

$$\mathcal{R}_n = \|u(x) - \mathcal{Q}_n u(x)\|_2, \quad x \in [a,b].$$

Theorem 4.1. *Suppose that $\mathcal{X}(\Psi)$ is a quasi-tight framelet system constructed using the OEP via the compactly supported function ϕ. For $s \geqslant -1$, assume that u satisfies the following decay equation, where*

$$D_u = \sum_{\ell=1}^{r}\sum_{j\geqslant 0}\sum_{k\in\mathbb{Z}} 2^{sj}\left|\left\langle u, \psi_{j,k}^{\ell}\right\rangle\right|^2 < \infty. \tag{4.4}$$

Thus,

$$\|u - \mathcal{Q}_n u\|_2 \leqslant D_u \mathcal{O}(2^{-(s+1)n}). \tag{4.5}$$

Proof. As any tight framelet system satisfies the Bessel inequality, and since $j \geqslant n$, we have

$$\begin{aligned}\|u - \mathcal{Q}_n u\|_2^2 = & \left\|\sum_{\ell=1}^{r}\sum_{j\geqslant n}\sum_{k\in\mathbb{Z}}\left\langle u, \psi_{j,k}^{\ell}\right\rangle \psi_{j,k}^{\ell}\right\|_2^2 \\ \leqslant & \sum_{\ell=1}^{r}\sum_{j\geqslant n}\sum_{k\in\mathbb{Z}}\left|\left\langle u, \psi_{j,k}^{\ell}\right\rangle\right|^2 \\ \leqslant & \sum_{\ell=1}^{r}\sum_{j\geqslant n}\sum_{k\in\mathbb{Z}}\frac{2^{(s+1)j}}{2^{(s+1)n}}\left|\left\langle u, \psi_{j,k}^{\ell}\right\rangle\right|^2.\end{aligned}$$

By the following fact

$$\left|\left\langle u, \psi_{j,k}^{\ell}\right\rangle\right| \leqslant \|u\|_\infty \left\|\psi_{j,k}^{\ell}\right\|_1 = \|u\|_\infty 2^{-j/2}\|\psi^{\ell}\|_1,$$

we have

$$\begin{aligned}\|u - \mathcal{Q}_n u\|_2^2 \leqslant & \|u\|_\infty \max_{\ell}\|\psi^{\ell}\|_1 \sum_{\ell=1}^{r}\sum_{j\geqslant n}\sum_{k\in\mathbb{Z}} 2^{-j}\left|\left\langle u, \psi_{j,k}^{\ell}\right\rangle\right| \\ \leqslant & \|u\|_\infty \max_{\ell}\|\psi^{\ell}\|_1 \sum_{\ell=1}^{r}\sum_{j\geqslant n}\sum_{k\in\mathbb{Z}} 2^{-j}\frac{2^{j(s+1)}}{2^{n(s+1)}}\left|\left\langle u, \psi_{j,k}^{\ell}\right\rangle\right| \\ \leqslant & \|u\|_\infty \max_{\ell}\|\psi^{\ell}\|_1 2^{-(s+1)n} D_u.\end{aligned}$$

Hence, the result is concluded. □

Table 1 The error results of Example 5.1.

n	System I	System II	System III	System IV
2	4.23×10^{-3}	4.95×10^{-6}	1.11×10^{-3}	4.43×10^{-6}
3	3.06×10^{-4}	5.38×10^{-7}	2.54×10^{-4}	3.19×10^{-7}
4	7.32×10^{-5}	6.01×10^{-8}	1.07×10^{-5}	2.44×10^{-9}
5	1.83×10^{-5}	2.27×10^{-9}	3.23×10^{-6}	1.23×10^{-10}
6	4.58×10^{-6}	2.65×10^{-10}	4.55×10^{-7}	2.81×10^{-11}
7	3.11×10^{-7}	5.06×10^{-11}	1.03×10^{-7}	3.01×10^{-12}
8	5.44×10^{-9}	4.76×10^{-12}	1.38×10^{-9}	5.75×10^{-13}
9	7.13×10^{-10}	1.32×10^{-12}	2.02×10^{-10}	7.95×10^{-14}
10	1.31×10^{-11}	8.27×10^{-13}	1.92×10^{-12}	2.02×10^{-15}

5. Numerical outputs

To demonstrate the efficiency and accuracy of the proposed method, we carry out in this part a series of numerical results. The numerical computations associated with the below examples are obtained via Mathematica Software.

Example 5.1. We consider the weakly singular Volterra-Fredholm integral equation given by:

$$u(x) = f(x) + \int_0^x \frac{1}{(x-t)^{\frac{1}{4}}} u(t)dt + \int_0^1 \frac{1}{(x-t)^{\frac{1}{4}}} u(t)dt.$$

where

$$\begin{aligned} f(x) = {} & \frac{1024x^{15/4}}{1155} - \frac{256x^{11/4}}{231} - \frac{512(x-1)^{3/4}x^3}{1155} - x^3 \\ & + \frac{256(x-1)^{3/4}x^2}{1155} + x^2 + \frac{48}{385}(x-1)^{3/4}x \\ & + \frac{16}{165}(x-1)^{3/4} \end{aligned}$$

and the exact solution is $u(x) = x^2(1-x)$.

In Table 1, the error $\mathcal{R}_n$ for different values of n is computed. Some illustrations for the graphs of the exact and approximate solutions and the error are depicted in Figs. 6–9. The graph of the convergence rate of the proposed method is depicted in Fig. 10.

Example 5.2. Here, we consider the following weakly singular Voterra-Fredholm integral equation

$$u(x) = f(x) + \int_0^x \frac{1}{(x-t)^{\frac{1}{3}}} u(t)dt + \int_0^1 \frac{1}{(x-t)^{\frac{1}{2}}} u(t)dt.$$

where

$$f(x) = x - \frac{9}{10}x^{5/3} - \frac{4}{3}x^{3/2} + \frac{2}{3}\sqrt{x-1} + \frac{4}{3}x\sqrt{x-1}.$$

Note that, the exact solution is $u(x) = x$.

In Table 2, the error $\mathcal{R}_n$ for different values of n is computed. Some illustrations for the graphs of the exact and approximate solutions and the error are depicted in Figs. 11 and 12. The graph of the convergence rate of the proposed method is depicted in Fig. 13.

Example 5.3. Now, we consider the following integral equation

$$u(x) = f(x) + \int_0^x \frac{1}{(x-t)^{\frac{1}{2}}} u(t)dt + \int_0^1 \frac{1}{(x-t)^{\frac{1}{2}}} u(t)dt.$$

where

$$f(x) = e^x(\sqrt{\pi}Erf(\sqrt{x-1}) - 2\sqrt{\pi}Erf(\sqrt{x}) + 1),$$

and, the exact solution is $u(x) = e^x$. The *error* function, $Erf(x)$, is defined by following equation

$$Erf(x) = \frac{2}{\sqrt{\pi}} \int_0^x e^{-t^2} dt.$$

For example when $n = 1, 2$ we provide, respectively, the explicit form of the approximate solutions, u_1 and u_2, where

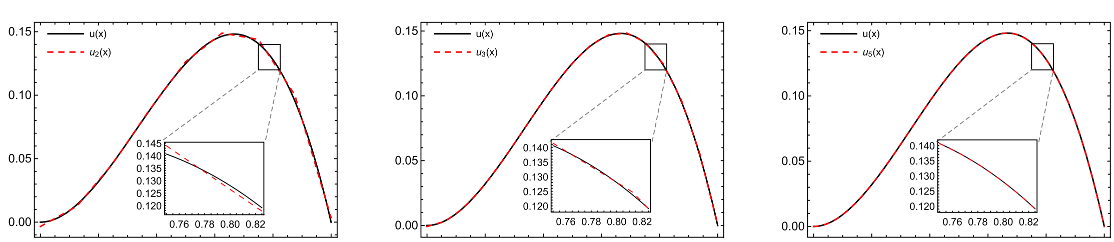

Fig. 6 The comparison between approximate and exact solutions of Example 5.1 using system I.

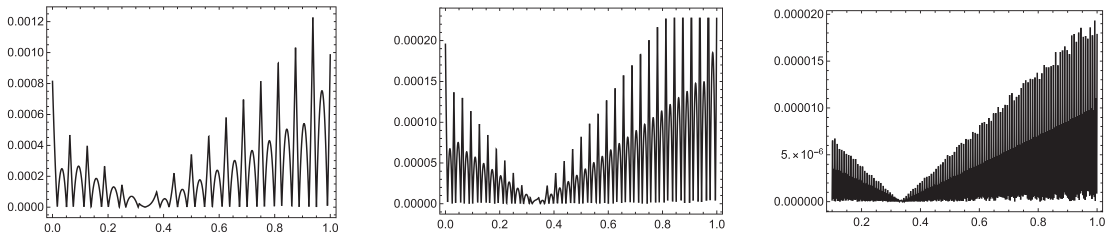

Fig. 7 The graphs of $\mathcal{E}_n(x), n = 3, 4, 6$, respectively, of Example 5.1 using System I.

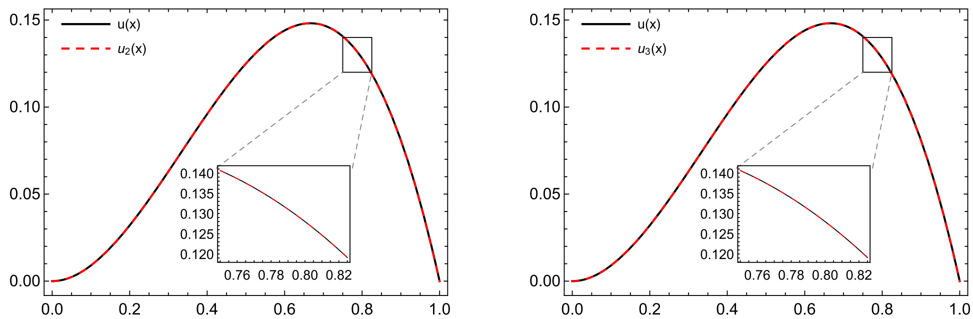

Fig. 8 The comparison between approximate and exact solutions of Example 5.1 using System II.

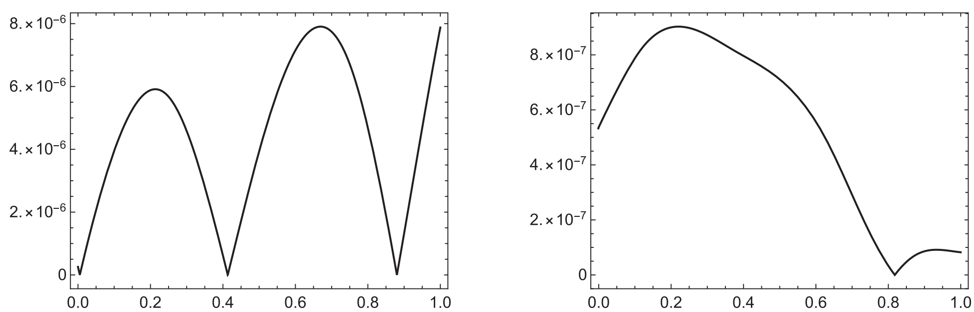

Fig. 9 The graphs of $\mathcal{E}_n(x), n = 2, 3$, respectively, of Example 5.1 using System II.

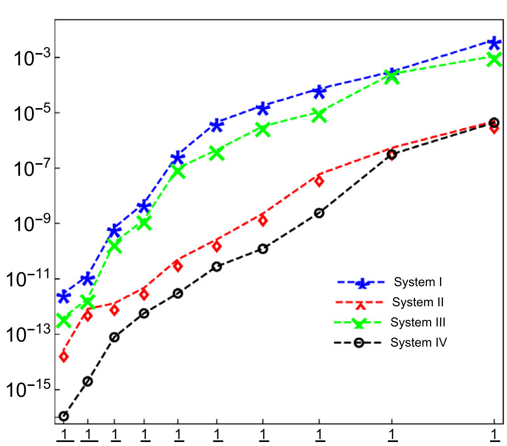

Fig. 10 Behavior of convergence rate for Examples 5.1 given in the log-log scale plot.

$$u_1(x) = \begin{cases} 0.690951 + 1.89068x, & 1/2 \leqslant x \leqslant 3/4, \\ 0.993324 + 1.14271x, & x \leqslant 1/4, \\ 0.347709 + 2.34834x, & x > 3/4, \\ 0.921710 + 1.42916x, & Otherwise, \end{cases} \tag{5.1}$$

and

$$u_2(x) = \begin{cases} 0.0997416 + 0.107440x, & x \leqslant 1/8, \\ 0.0195960 + 0.2512570x, & x \geqslant 7/8, \\ 0.0439263 + 0.223451x, & 3/4 \leqslant x < 7/8, \\ 0.0625969 + 0.198556x, & 5/8 \leqslant x < 3/4, \\ 0.0760292 + 0.177065x, & 1/2 \leqslant x < 5/8, \\ 0.0873838 + 0.154356x, & 3/8 \leqslant x < 1/2, \\ 0.0941087 + 0.136422x, & 1/4 \leqslant x < 3/8, \\ 0.0981289 + 0.120342x, & Otherwise. \end{cases} \tag{5.2}$$

In Table 3, the error $\mathcal{R}_n$ for different values of n is computed. Some illustrations for the graphs of the exact and approximate solutions and the error are depicted in Figs. 14

Table 2 The error results of Example 5.2.

n	System I	System II	System III	System IV
2	2.55×10^{-3}	1.45×10^{-6}	1.75×10^{-3}	1.54×10^{-6}
3	3.11×10^{-4}	5.56×10^{-7}	4.32×10^{-4}	1.45×10^{-7}
4	1.02×10^{-5}	2.75×10^{-9}	8.01×10^{-6}	1.77×10^{-9}
5	4.63×10^{-6}	1.01×10^{-9}	2.33×10^{-6}	7.57×10^{-10}
6	2.34×10^{-7}	7.11×10^{-10}	1.01×10^{-7}	4.76×10^{-10}
7	3.83×10^{-8}	2.54×10^{-11}	1.24×10^{-8}	2.84×10^{-12}
8	7.31×10^{-10}	4.35×10^{-12}	2.45×10^{-10}	4.56×10^{-13}
9	5.30×10^{-11}	2.68×10^{-12}	2.75×10^{-11}	5.60×10^{-14}
10	1.12×10^{-11}	2.35×10^{-13}	4.67×10^{-12}	1.09×10^{-15}

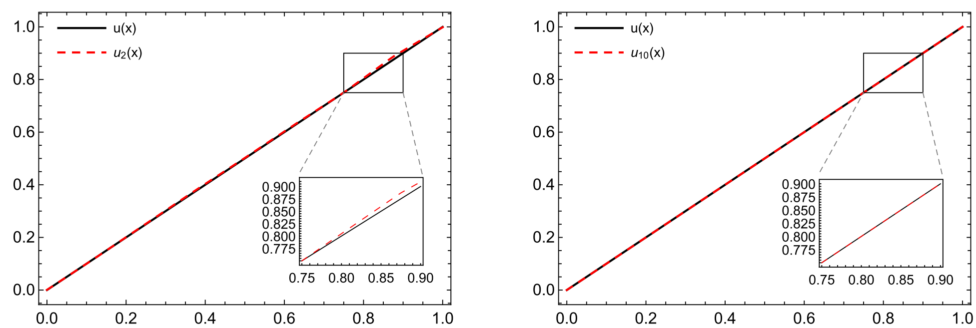

Fig. 11 The comparison between approximate and exact solutions of Example 5.2 using System I.

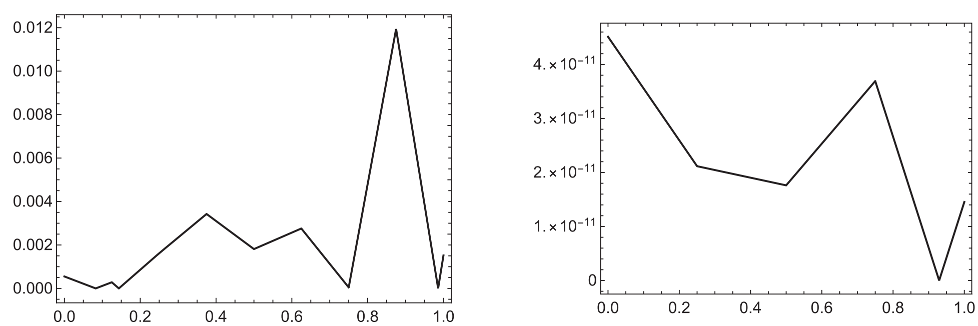

Fig. 12 The graphs $\mathcal{E}_n(x)$ when $n = 2, 10$ of Example 5.2 using System I, respectively.

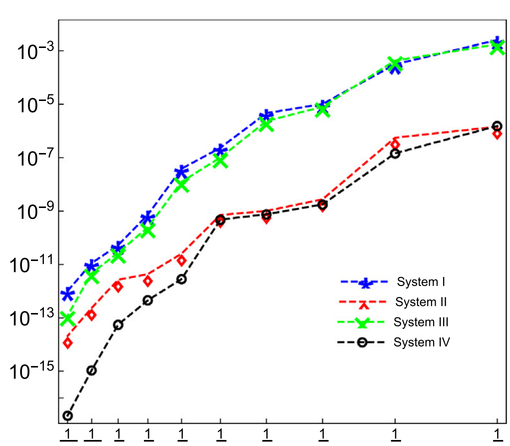

Fig. 13 Behavior of convergence rate for Examples 5.2 given in the log-log scale plot.

and 15. The graph of the convergence rate of the proposed method is depicted in Fig. 16.

6. Conclusion

This paper adopts a quasi-affine tight framelets collocation-based method to solve one of the most important linear weakly singular-mixed Volterra-Fredholm integral equations using a tight framelet. We converted the integral system that was obtained by the collocation-based method to a linear system of equations which is easy to solve. We solved this system to get an approximated solution in a series of three examples. The numerical results obtained in the tables and graphs confirm the accuracy and efficiency of the method.

We noted that the approximated results in Figs. 6, 8, 11, and 14 agree perfectly with the exact solutions of the WSVFIEs presented. The approximate solutions are getting

Table 3 The error results of Example 5.3.

n	System I	System II	System III	System IV
2	5.93×10^{-3}	3.06×10^{-6}	1.01×10^{-3}	2.77×10^{-6}
3	6.82×10^{-4}	2.56×10^{-7}	1.79×10^{-4}	6.88×10^{-8}
4	7.57×10^{-5}	6.54×10^{-8}	2.67×10^{-6}	3.45×10^{-9}
5	8.23×10^{-6}	2.45×10^{-10}	0.22×10^{-6}	0.78×10^{-10}
6	4.92×10^{-7}	2.34×10^{-10}	2.44×10^{-8}	1.98×10^{-11}
7	5.31×10^{-8}	5.96×10^{-11}	1.02×10^{-8}	2.23×10^{-12}
8	6.82×10^{-9}	8.51×10^{-12}	0.31×10^{-9}	3.55×10^{-14}
9	7.28×10^{-11}	6.04×10^{-13}	1.61×10^{-11}	1.08×10^{-15}
10	2.03×10^{-12}	2.23×10^{-14}	0.17×10^{-12}	0.41×10^{-16}

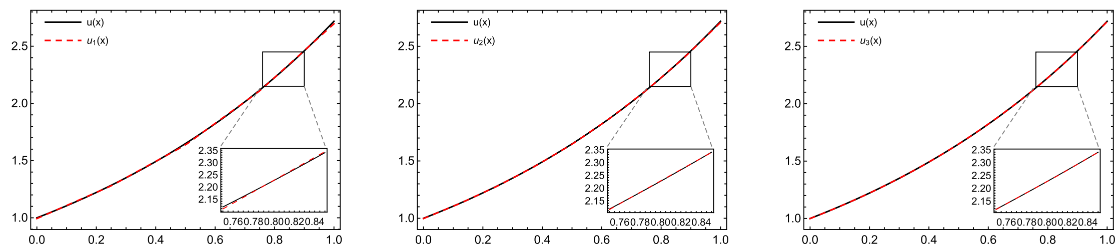

Fig. 14 The comparison between approximate and exact solutions of Example 5.3 using System I.

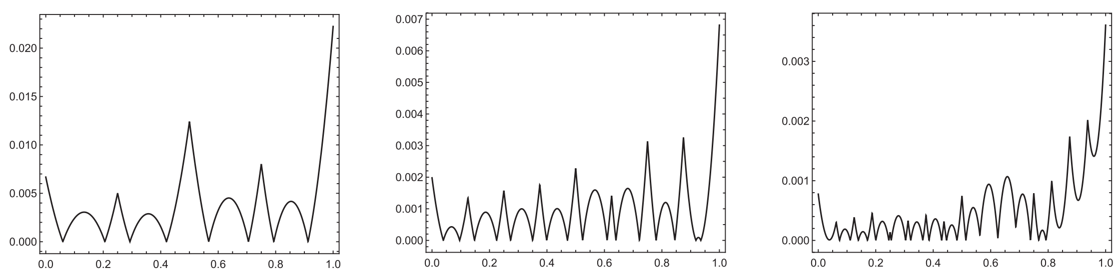

Fig. 15 The graphs of $\mathcal{E}_n(x), n = 1, 2, 3$, respectively, of Example 5.3 using System I.

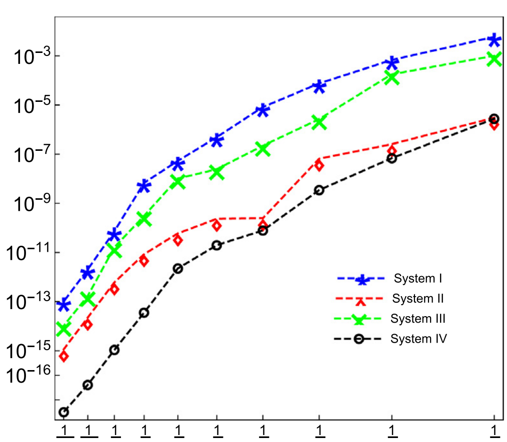

Fig. 16 Behavior of convergence rate for Examples 5.3 given in the log-log scale plot.

closer and closer to the exact one as we increase the number n. The error history and the convergence behavior are displayed in Figs. 10, 13, 16, and in Figs. 7, 9, 12, and 15, respectively, where we see suboptimal convergence rates and a satisfactory agreement is observed with respect to the theoretical predictions.

It turns out that, enhancing the order level of the vanishing moments for the underlying refinable function being handled to construct the framelet system, would result an increase in the accuracy orders, better approximation fitting as well as the efficiency of the method.

Declaration of Competing Interest

The authors declare that they have no known competing financial interests or personal relationships that could have appeared to influence the work reported in this paper.

Acknowledgments

We would like to thank the anonymous reviewers for their valuable comments to improve the presentation and quality of the paper.

References

[1] P. Schiavane, C. Constanda, A. Mioduchowski, Integral Methods in Science and Engineering, Birkhuser, Boston, 2002.
[2] B. Semetanian, On an integral equation for axially symmetric problem in the case of an elastic body containing an inclusion, J. Comput. Appl. Math. 200 (2007) 12–20.
[3] M. Jaswon, G.T. Symm, Integral Equation Methods in Potential Theory and Elastostatics, Academic Press, London, 1977.
[4] R. Bagley, P.J. Torvik, Fractional calculus: a different approach to the analysis of viscoelastically damped structures, AIAA J. 21 (1983) 741–748.
[5] G. Symm, An integral equation method in conformal mapping, Numer. Math. 9 (1966) 250–258.
[6] E. Hopf, Mathematical Problems of Radiative Equilibrium, Stechert-Hafner Service Agency, NewYork, 1964.
[7] A.M. Wazwaz, Linear and Nonlinear Integral Equations: Methods and Applications, Higher Education Press and Springer Verlag, Heidelberg, 2011.
[8] R. Hilfer, Applications of Fractional Calculus in Physics, World Scientific Pub. Co., Pte. Ltd, Singapore, 2000.
[9] P. Kythe, P. Puri, Computational Methods for Linear Integral Equations, Birkhauser, Boston, 2002.
[10] A. Atangana, Fractional discretization: The African's tortoise walk 130 (2020) 109399.
[11] A. Atangana A., D. Baleanu, New fractional derivatives with non-local and non-singular kernel: theory and application to heat transfer model, Therm. Sci. 20 (2016) 763–769.
[12] J. Singh, D. Kumar, Z. Hammouch, A. Atangana, A fractional epidemiological model for computer viruses pertaining to a new fractional derivative, Appl. Math. Comput. 316 (2018) 504–515.
[13] A. Atangana, T. Alkahtani, Analysis of the Keller-Segel model with a fractional derivative without singular kernel, Entropy 17 (2015) 4439–4453.
[14] T. Sulaiman, H. Bulut, H. Baskonus, Optical solitons to the fractional perturbed NLSE in nano-fibers, Discrete Continuous Dyn. Syst.-S 13 (2020) 925–936.
[15] G. Yel, T. Sulaiman, H. Baskonus, On the complex solutions to the $(3+1)$-dimensional conformable fractional modified KdV–Zakharov–Kuznetsov equation, Mod. Phys. Lett. B 2050069 (2020) 1–17.
[16] W. Gao, P. Veeresha, D.G. Prakasha, H. Baskonus, G. Yel, A powerful approach for fractional Drinfeld–Sokolov–Wilson equation with Mittag-Leffler law, Alexand. Eng. J. 58 (2019) 1301–1311.
[17] W. Gao, G. Yel, H. Baskonus, C. Cattani, Complex solitons in the conformable $(2+1)$-dimensional Ablowitz-Kaup-Newell-Segur equation, Aims Math. 5 (2020) 507–521.
[18] A. Prakash, M. Goyal, H. Baskonus, S. Gupta, A reliable hybrid numerical method for a time dependent vibration model of arbitrary order, Aims Math. 5 (2020) 979–1000.
[19] D. Kumar, J. Singh, D. Baleanu, S. Rathore, Analysis of regularized long-wave equation associated with a new fractional operator with Mittag-Leffler type kernel, Physica A 492 (2018) 155–167.
[20] J. Singh, D. Kumar, D. Baleanu, S. Rathore, On the local fractional wave equation in fractal strings, Math. Methods Appl. Sci. 42 (5) (2019) 1588–1595.
[21] D. Kumar, J. Singh, D. Baleanu, A new numerical algorithm for fractional Fitzhugh-Nagumo equation arising in transmission of nerve impulses, Nonlinear Dyn. 91 (2018) 307–317.
[22] M. Ahmadabadi, H. Dastjerdi, Tau approximation method for the weakly singular Volterra-Hammerstein integral equations, App. Math. Comp. 285 (2015) 241–247.
[23] I. Lifanov, L.N. Poltavskii, G.M. Vainikko, Hypersingular Integral Equations and their Applications, CRC Press, New Jersey, 2004.
[24] H. Du, G. Zhao, C. Zhao, Reproducing Kernel method of solving Fredholm integro-differential equations with weakly singularity, J. Comput. Appl. Math. 255 (2013) 122–132.
[25] A. Pedas, E. Tamme, Discrete Galerkin method for Fredholm integro-differential equations with weakly singular kernels, J. Comput. Appl. Math. 213 (2008) 111–126.
[26] P. Sahu, S. Ray, Legendre wavelets operational method for the numerical solutions of nonlinear Volterra integro-differential equations system, Appl. Math. Comput. 256 (2015) 715–723.
[27] M. Heydari, M.R. Hooshmandasl, Legendre wavelets method for solving fractional partial differential equations with Dirichlet boundary conditions, Appl. Math. Comput. 234 (2014) 267–276.
[28] Z. Meng, L.F. Wang, H. Li, W. Zhang, Legendre wavelets method for solving fractional integro-differential equations, Int. J. Comput. Math. 92 (6) (2015) 1275–1291.
[29] T.A. Burton, Volterra Integral and Differential Equations, Elsevier B.V., Netherlands, 2005.
[30] H. Brunner, Collocation Method for Volterra Integral and Related Functional Equations, Cambridge University Press, Cambridge, 2004.
[31] L.M. Delves, J.L. Mohamed, Computational Methods for Integral Equations, Cambridge University Press, Cambridge, 1985.
[32] M. Sezer, Taylor polynomial solution of Volterra integral equations Int, J. Math. Edu. Sci. Tech. 25 (5) (1994) 625.
[33] S. Yalnba Taylor, polynomial solutions of nonlinear Volterra-Fredholm integral equations, Appl. Math. Comput. 127 (2002) 195–206.
[34] A. Akyüz-Daolu, M. Sezer, Chebyshev polynomial solutions of systems of higher-order linear Fredholh-Volterra integro-differential equations, J. Franklin Inst. 342 (2005) 688–701.
[35] M. Ghasemi, M. Tavassoli Kajani, E. Bobolian Numerical solutions of the nonlinear Volterra-Fredholm integral equations by using homotopy perturbation method, Appl. Math. Comput. 188 (2007) 446–449.
[36] J. Biazar, H. Ghazvini, He's homotopy perturbation method for solving system of Volterra integral equations of the second kind, Chaos Solitons Fract. 39 (2) (2009) 770–777.
[37] A. Tahmasbi, O.S. Fard, Numerical solution of linear Volterra integral equations system of the second kind, Appl. Math. 201 (2008) 547–552.
[38] M. Mohammad, E.B. Lin, Gibbs phenomenon in tight framelet expansions, Commun. Nonlinear Sci. Numer. Simul. 55 (2018) 84–92.
[39] M. Mohammad, E.B. Lin, Gibbs effects using Daubechies and Coiflet tight framelet systems, Contemp. Math. AMS 706 (2018) 271–282.
[40] M. Mohammad, Special B-spline tight framelet and it's applications, J. Adv. Math. Comput. Sci. 29 (2018) 1–18.
[41] M. Mohammad, On the gibbs effect based on the quasi-affine dual tight framelets system generated using the mixed oblique extension principle, Mathematics 7 (2019).
[42] M. Mohammad, F. Howari, G. Acbas, Y. Nazzal, F. AlAydaroos, Wavelets based simulation and visualization approach for unmixing of hyperspectral data, Int. J. Earth Environ. Sci. 3 (2018).
[43] M. Mohammad, Biorthogonal-wavelet-based method for numerical solution of Volterra integral equations M Mohammad, Entropy 21 (2019) 1098.
[44] M. Mohammad, A numerical solution of fredholm integral equations of the second kind based on tight framelets generated by the oblique extension principle, Symmetry 11 (2019) 854.

[45] I. Daubechies, B. Han, A. Ron, Z. Shen, Framelets: MRA-based constructions of wavelet frames, Appl. Comput. Harmon. 14 (2003) 1–46.

[46] I. Daubechies, A. Grossmann, Y. Meyer, Painless nonorthogonal expansions, J. Math. Phys. 27 (162) (1986) 1271–1283.

[47] I. Daubechies, Ten Lectures on Wavelets, SIAM, Philadelphia, 1992.

[48] B. Dong, Z. Shen, MRA Based Wavelet Frames and Applications, IAS Lecture Notes Series, Summer Program on "The Mathematics of Image Processing", Park City Mathematics Institute, 2010.

[49] O. Christensen, An Introduction to Frames and Riesz Bases, Birkhauser, Boston, 2003.

[50] B. Han, Framelets and Wavelets: Algorithms, Analysis, and Applications. Applied and Numerical Harmonic Analysis, Birkhäuser/Springer, Cham, 2017.

[51] A. Ron, Z. Shen, Affine systems in $L^2(\mathbb{R}^d)$: the analysis of the analysis operators, J. Funct. Anal. 148 (1997) 408–447.